Sensing waveforms design for distributed OFDM radars

Xinghe Li, Jinyang He, Hongzhi Guo, Dong Xu, Huiyong Li and Ziyang Cheng
School of Information and Communication Engineering, *UESTC*, Chengdu 611731, China
Email: xinghe_lee@126.com; jinyanghe@126.com; hongz_guo@126.com

***Abstract*—This paper investigates the problem of the collaborative sensing sequences for distributed orthogonal frequency-division multiplexing (OFDM) base stations (radars) with aim of low auto-correlation and cross-correlation levels. Considering the constraints of characteristics of OFDM waveforms, peak-to-average power ratio (PAPR) and energy of the OFDM sequences, the optimization problem is established by minimizing the weighted integrated sidelobe level (WISL). Since the resultant problem involves a nonconvex fourth-order objective and a nonconvex constraint, it is difficult to obtain a closed-form solution. Towards that ends, an efficient iterative method based on the alternating direction method of multipliers (ADMM) algorithm is devised to solve the problem. Finally, the WISL property of the designed sequences is verified by numerical simulations.**

***Index Terms*—Collaborative OFDM sequences, distributed radars, time-frequency structure constraint, weighted integrated sidelobe level (WISL)**

I. Introduction

In recent years, distributed sensing base stations have garnered increasing research interest due to their ability to achieve spatial diversity gains through spatial multiplexing [1]. In the distributed sensing base stations, the distribution of stations at different spatial locations gives rise to different angles relative to the target, thereby achieving spatial multiplexing gain and geometric gain. Distributed radar typically transmits orthogonal signals to distinguish the transmitted signals from different radar stations by matching and separating the received data, thereby preserving target information more effectively [2].

Typically, effective orthogonal signal energy emphasizes the design of waveforms with low autocorrelation sidelobes after distance compression [3] [4]. Early orthogonal code design mainly focused on the construction of phase codes with low autocorrelation properties. For example, researchers in [5] used a genetic algorithm to optimize orthogonal polyphase codes. With the development of optimization theory, the design of orthogonal waveforms with continuous phase codes has also attracted widespread attention. In [6] [7], a weighted new cyclic algorithms was proposed to indirectly optimize the weighted integrated sidelobe level (WISL) of the waveform. In [8], a nonlinear alternating direction method of multipliers (Nonlinear-ADMM) was proposed to directly optimize the WISL of the waveform, achieving lower correlation sidelobe levels compared to [6]. However, these methods mainly address situations involving constant modulus waveforms. For non-constant modulus waveforms, such as orthogonal frequency division multiplexing (OFDM) signals, they are no longer applicable [9].

Compared to traditional radar waveforms such as linear frequency modulation (LFM), OFDM waveforms offer advantages such as higher range resolution [10], lower Doppler sensitivity [11], stronger anti-jamming capabilities [12], and waveform diversity [13], making them suitable for radar detection. However, the phases of the subcarriers in an OFDM waveform are independent in the frequency domain, which means they can be combined constructively or destructively [14]. This results in a large dynamic range for the time-domain OFDM waveform, and its peak-to-average power ratio (PAPR) is typically high [15]. In [16] [17], a joint transceiver design method is proposed to minimize the ratio between the peak value to integrated sidelobe level under the PAPR constraint, which achieves a trade-off between sidelobe performance and PAPR performance. However, these methods are designed only for single OFDM waveform designs and do not consider the design of orthogonal waveforms for distributed OFDM base stations.

Based on the above analysis, this study investigates the design of distributed OFDM radar waveforms with low cross-correlation sidelobes for cooperative sensing. Firstly, the WISL formulation of distributed OFDM base stations waveforms is derived and used as the objective function to establish an optimization problem, while also considering constraints such as time-frequency structure, PAPR, and energy allocation. A solution process based on the alternating direction method of multipliers (ADMM) method is proposed according to the above analysis. Finally, simulation results demonstrate the low cross-correlation sidelobe performance of the designed distributed OFDM waveforms.

Notation: $\mathbf{a}$ and $\mathbf{A}$ denote a vector and a matrix, respectively. $(\cdot)^*$, $(\cdot)^T$ and $(\cdot)^H$ separately stand for the conjugate, transpose and conjugate transpose operators. $\mathbb{C}^{N\times N}$ represents the sets of $N \times N$ complex-valued matrices. $\mathrm{vec}(\mathbf{A})$ denotes the vectorization of matrix $\mathbf{A}$. $\mathbf{I}_N$ denotes the $N \times N$ identity matrix and $\otimes$ denotes Kronecker product, respectively.

II. Signal Model and Problem Formulation

In this section, we first present the signal model for the distributed OFDM base stations considered in this study. Sub-

This work was supported in part by the National Natural Science Foundation of China under Grant 62371096, Grant 62001084, and Grant 62231006; in part by Sichuan Science and Technology Program under Grant 2023NSFSC1385; and in part by the Sichuan Province Science and Technology Plan under Grant 2023ZHJY0011.

sequently, an optimization model is formulated with the minimization of WISL as the objective function, time-frequency structure, PAPR, and energy constraints as conditions.

A. Signal Model

Assume the number of base stations (BSs) in the distributed OFDM base stations is M and the OFDM waveform transmitted by each BS contains N subcarriers. The frequency-domain signals from all stations can be represented as $\mathbf{s} = [\mathbf{s}_1^T, \mathbf{s}_2^T ..., \mathbf{s}_M^T]^T$, where $\mathbf{s_m} = [s_{m1}, \ldots, s_{mN}]^T$ denotes the frequency-domain signal of the m-th station. Similarly, the time-domain OFDM sensing waveform for the M stations can be represented as $\mathbf{x} = [\mathbf{x}_1^T, \mathbf{x}_2^T ..., \mathbf{x}_M^T]^T$, where $\mathbf{x}_m = [x_m(1), \ldots, x_m(N)]^T$. The time-frequency domain signal of the m-th station satisfies the following relationship:

$$\mathbf{x}_m = \mathbf{F}^H \mathbf{s}_m \tag{1}$$

where $\mathbf{F} \in \mathbb{C}^{N \times N}$ is the discrete Fourier transformation (DFT) matrix (scaled by $1/N$)

$$\mathbf{F} = \frac{1}{N} \begin{bmatrix} 1 & 1 & \cdots & 1 \\ 1 & e^{-j\frac{2\pi}{N}\cdot 1} & \cdots & e^{-j\frac{2\pi}{N}\cdot(N-1)} \\ \vdots & \vdots & \ddots & \vdots \\ 1 & e^{-j\frac{2\pi}{N}\cdot(N-1)} & \cdots & e^{-j\frac{2\pi}{N}\cdot(N-1)(N-1)} \end{bmatrix} \tag{2}$$

Therefore, the time-frequency relationship of all BSs can be written as

$$\mathbf{x} = (\mathbf{I}_M \otimes \mathbf{F}^H)\mathbf{s} \tag{3}$$

For distributed radar cooperative sensing waveform design, it is generally desired that the designed waveforms exhibit low autocorrelation and cross-correlation sidelobes. According to [8], the integrated sidelobe level (ISL) for distributed OFDM radar can be defined by the following equation:

$$\begin{aligned} \varepsilon_r = &\sum_{m=1}^{M} \sum_{n=-N+1}^{N-1} |r_{mm}(n)|^2 \\ &+ \sum_{m_1=1}^{M} \sum_{m_2=1}^{M} \sum_{n=-N+1}^{N-1} |r_{m_1 m_2}(n)|^2 \end{aligned} \tag{4}$$

where $r_{mm}(n)$ represents the n-th sample of the autocorrelation of the m-th BS station and $r_{m_1 m_2}(n)$ represents the n-th sample of the time-domain cross-correlation function of the m_1-th BS and m_2-th BS, which is defined as:

$$\begin{aligned} r_{mm}(n) &= \sum_{k=n+1}^{N} x_m(k) x_m^*(k-n) \\ r_{m_1 m_2}(n) &= \sum_{k=n+1}^{N} x_{m_1}(k) x_{m_2}^*(k-n) \end{aligned} \tag{5}$$

In practical applications, the WISL is typically expressed in the following form:

$$\begin{aligned} \tilde{\varepsilon}_r = &\gamma_0^2 \sum_{m_1=1}^{M} \sum_{\substack{m_2=1 \\ m_2 \neq m_1}}^{M} |r_{m_1 m_2}(0)|^2 \\ &+ \sum_{\substack{n=-N+1 \\ n \neq 0}}^{N-1} \gamma_n^2 \left(\sum_{m_1=1}^{M} \sum_{m_2=1}^{M} |r_{m_1 m_2}(n)|^2 \right) \end{aligned} \tag{6}$$

Eq.(6) can be concisely expressed in matrix form as:

$$\varepsilon_r = \frac{1}{2N} \sum_{p=0}^{2N-1} \left\| \mathbf{X}^H \mathbf{C}_p \mathbf{X} \right\|_2^2 + \mathrm{c} \tag{7}$$

where c represents a constant. $\mathbf{X} = [\mathbf{x}_1, \mathbf{x}_2 ..., \mathbf{x}_M] \in \mathbb{C}^{N \times M}$; $\mathbf{C}_p \triangleq \mathbf{A}_p^H \Gamma \mathbf{A}_p$, $\mathbf{A_p} = \mathrm{Diag}\left(\left[1, e^{-j\omega_p}, \cdots, e^{-j\omega_p (N-1)} \right] \right)$, $\omega_p = 2\pi p / 2N, p = 0, 1, \ldots, 2N-1$, where $\mathbf{A_p}$ means the diagonal matrix of the frequency relationship between subcarriers and $\mathbf{\Gamma}$ means the matrix of the weighted coefficient.

$$\mathbf{\Gamma} = \begin{bmatrix} \gamma_0 & \gamma_1 & \cdots & \gamma_{N-1} \\ \gamma_1 & \gamma_0 & \ddots & \vdots \\ \vdots & \ddots & \ddots & \gamma_1 \\ \gamma_{N-1} & \cdots & \gamma_1 & \gamma_0 \end{bmatrix} \tag{8}$$

B. Problem Formulation

In the distributed OFDM radar cooperative sensing waveform design problem, we aim to design waveforms with low autocorrelation and cross-correlation sidelobe levels while satisfying the following constraints:

1) Energy constraint;

2) The time-frequency relationship of the OFDM waveform;

3) Limit the PAPR of the time domain waveform to improve the efficiency of the transmitter.

Therefore, the distributed OFDM radar cooperative sensing waveform design problem can be modeled as

$$\begin{aligned} \min_{\mathbf{X},\mathbf{S},\mathbf{x}} \quad & \sum_{p=0}^{2N-1} \left\| \mathbf{X}^H \mathbf{C}_p \mathbf{X} \right\|_2^2 \\ \mathbf{s.t.} \quad & \mathbf{X} = \mathbf{F}^H \mathbf{S}, \mathbf{x} = \mathrm{vec}\,(\mathbf{X}) \\ & |x_{mn}|^2 \leq \eta P, m = 1, 2, \ldots, M, n = 1, \ldots, N \\ & \mathbf{x}^H \mathbf{E}_m \mathbf{x} = 1, m = 1, \ldots, M \end{aligned} \tag{9}$$

where η is a parameter that controls the level of PAPR and P is the average signal power. $\mathbf{E}_m \in {}^{MN \times MN}$ is the selection matrix, whose (i,i)-th element $(i = 1 + (m-1) \times N : m \times N$ is $1)$, and the other elements are 0.

Since the problem (9) involves a quartic objective function with respect to $\mathbf{X}$ and quadratic equality constraints with respect to $\mathbf{x}$, it constitutes a non-convex problem. Therefore, this paper designs a method based on ADMM to solve this problem.

III. Proposed Method for Collaborative Sensing Waveform Design

Since the objective function in problem (9) is quartic with respect to $\mathbf{X}$ and is difficult to solve, the time-frequency relationship of OFDM waveforms $\mathbf{X} = \mathbf{F}^H\mathbf{S}$ is utilized to replace one $\mathbf{X}$ with $\mathbf{S}$. As a result,the problem (9) is transformed into a quadratic optimization problem with respect to variables $\mathbf{X}$ and $\mathbf{S}$ respectively.

$$\begin{aligned}\min_{\mathbf{X},\mathbf{S},\mathbf{x},\mathbf{s}} \quad & \sum_{p=0}^{2N-1} \left\|\mathbf{X}^H\mathbf{C}_p\mathbf{F}^H\mathbf{S}\right\|_2^2 \\ \text{s.t.} \quad & \mathbf{x} = \left(\mathbf{I}_M \otimes \mathbf{F}^H\right)\mathbf{s}, \quad \mathbf{x} = \mathrm{vec}(\mathbf{X}), \\ & |x_{mn}|^2 \le \rho P, \quad m = 1,2,\ldots,M,\ n = 1,\ldots,N, \\ & \mathbf{x}^H\mathbf{E}_m\left(\mathbf{I}_M \otimes \mathbf{F}^H\right)\mathbf{s} = 1, \quad m = 1,\ldots,M.\end{aligned} \tag{10}$$

To solve the problem (10) within the ADMM framework, we treat the equality constraints as penalty terms, thereby constructing the augmented Lagrangian function for the above problem as follows:

$$\begin{aligned}\mathcal{L}(\mathbf{x},\mathbf{s},\mathbf{u},v) = & \sum_{p=0}^{2N-1} \left\|\mathbf{X}^H\mathbf{C}_p\mathbf{F}^H\mathbf{S}\right\|_2^2 \\ & + \frac{\rho_u}{2}\left\|\mathbf{x} - \left(\mathbf{I}_M \otimes \mathbf{F}_I\right)\mathbf{s} + \mathbf{u}\right\|_2^2 \\ & + \frac{\rho_v}{2}\sum_{m=1}^{M}\left\|\mathbf{x}^H\mathbf{E}_m\left(\mathbf{I}_M \otimes \mathbf{F}^H\right)\mathbf{s} - 1 + v_m\right\|_2^2.\end{aligned} \tag{11}$$

By minimizing $\mathcal{L}(\mathbf{x},\mathbf{s},\mathbf{u},v)$ to update the variables, the $(k+1)$-th iteration consists of the following update steps (12).

$$\begin{aligned}\mathbf{x}^{(k+1)} &= \underset{|x_{mn}|^2 \le \rho P}{\arg\min}\ \mathcal{L}\left(\mathbf{x},\mathbf{s}^{(k)},\mathbf{u}^{(k)},v^{(k)}\right) \\ \mathbf{s}^{(k+1)} &= \underset{|\mathbf{s}_{mn}|=1}{\arg\min}\ \mathcal{L}\left(\mathbf{x}^{(k+1)},\mathbf{s},\mathbf{u}^{(k)},v^{(k)}\right) \\ \mathbf{u}^{(k+1)} &= \mathbf{u}^{(k)} + \mathbf{x}^{(k+1)} - \left(\mathbf{I}_M \otimes \mathbf{F}^H\right)\mathbf{s}^{(k+1)} \\ v_m^{(k+1)} &= v_m^{(k)} + \left(\mathbf{x}^{(k+1)}\right)^H\mathbf{E}_m\left(\mathbf{I}_M \otimes \mathbf{F}^H\right)\mathbf{s}^{(k+1)} - 1\end{aligned} \tag{12}$$

In the sequel, the solutions to problem (9) are presented.

1) Update $\mathbf{x}$*:*

To update $\mathbf{x}$, we first transform the first term in equation (11)

$$\begin{aligned}\left\|\mathbf{X}^H\mathbf{C}_p\mathbf{F}^H\mathbf{S}\right\|_2^2 &= \mathrm{vec}^H\left(\mathbf{S}^H\mathbf{F}\mathbf{C}_p\mathbf{X}\right)\mathrm{vec}\left(\mathbf{S}^H\mathbf{F}\mathbf{C}_p\mathbf{X}\right) \\ &= \mathbf{x}^H\left(\mathbf{I}_M \otimes \mathbf{S}^H\mathbf{F}\mathbf{C}_p\right)^H\left(\mathbf{I}_M \otimes \mathbf{S}^H\mathbf{F}\mathbf{C}_p\right)\mathbf{x} \\ &= \mathbf{x}^H\left(\mathbf{I}_M \otimes \mathbf{C}_p^H\mathbf{F}^H\mathbf{S}\mathbf{S}^H\mathbf{F}\mathbf{C}_p\right)\mathbf{x} \\ &= \mathbf{x}^H\mathbf{D}_p\left(\mathbf{S}\right)\mathbf{x}\end{aligned} \tag{13}$$

where $\mathbf{D}_p\left(\mathbf{S}\right) = \mathbf{I}_M \otimes \mathbf{C}_p^H\mathbf{F}^H\mathbf{S}\mathbf{S}^H\mathbf{F}\mathbf{C}_p$.

Substituting (13) into (11), and taking the derivative of the augmented Lagrangian function with respect to the variable $\mathbf{x}^*$, we obtain:

$$\begin{aligned}\frac{\partial\mathcal{L}}{\partial\mathbf{x}^*} = & \sum_{p=0}^{2N-1} 2\mathbf{D}_p\left(\mathbf{S}^{(k)}\right)\mathbf{x} \\ & + \rho_u\left(\mathbf{x} - \left(\mathbf{I}_M \otimes \mathbf{F}^H\right)\mathbf{s}^{(k)} + \mathbf{u}^{(k)}\right) \\ & + \rho_v\sum_{m=1}^{M}\mathbf{E}_m\left(\mathbf{I}_M \otimes \mathbf{F}^H\right)\mathbf{s}^{(k)} \\ & \left[\left(\mathbf{s}^{(k)}\right)^H\left(\left(\mathbf{I}_M \otimes \mathbf{F}^H\right)^H\mathbf{E}_m^H\mathbf{x} - 1 + \left(v_m^{(k)}\right)^*\right)\right]\end{aligned} \tag{14}$$

Let the derivative be zero, and then we obtain

$$\begin{aligned}\mathbf{x} = & \left[\sum_{p=0}^{2N-1} 2\mathbf{D}_p\left(\mathbf{S}^{(k)}\right) + \rho_u\mathbf{I} + \rho_v\sum_{m=1}^{M}\mathbf{E}_m\left(\mathbf{I}_M \otimes \mathbf{F}^H\right)\mathbf{s}^{(k)}\right. \\ & \left.\times\left(\mathbf{s}^{(k)}\right)^H\left(\mathbf{I}_M \otimes \mathbf{F}^H\right)^H\mathbf{E}_m^H\right]^{-1} \\ & \cdot\left\{\rho_u\left(\left(\mathbf{I}_M \otimes \mathbf{F}^H\right)\mathbf{s}^{(k)} - \mathbf{u}^{(k)}\right)\right. \\ & \left.+\rho_v\sum_{m=1}^{M}\mathbf{E}_m\left(\mathbf{I}_M \otimes \mathbf{F}^H\right)\mathbf{s}^{(k)}\left(1 - \left(v_m^{(k)}\right)^*\right)\right\}\end{aligned} \tag{15}$$

By projecting the result of eq. (15) onto the feasible set, x is updated as follows

$$x_{mn}^{(k+1)} = \begin{cases}\frac{\sqrt{\eta P}x_{mn}}{|x_{mn}|}, & \text{if } |x_{mn}|^2 > \eta P \\ x_{mn}, & \text{otherwise}\end{cases} \tag{16}$$

2) Update $\mathbf{s}$*:*

Similarly, to update $\mathbf{s}$, the first term in equation (11) is transformed into:

$$\begin{aligned}\left\|\mathbf{X}^H\mathbf{C}_p\mathbf{F}^H\mathbf{S}\right\|_2^2 &= \mathrm{vec}^H\left(\mathbf{X}^H\mathbf{C}_p\mathbf{F}^H\mathbf{S}\right)\mathrm{vec}\left(\mathbf{X}^H\mathbf{C}_p\mathbf{F}^H\mathbf{S}\right) \\ &= \mathbf{s}^H\left(\mathbf{I}_M \otimes \mathbf{X}^H\mathbf{C}_p\mathbf{F}^H\right)^H \\ &\quad\times\left(\mathbf{I}_M \otimes \mathbf{X}^H\mathbf{C}_p\mathbf{F}^H\right)\mathbf{s} \\ &= \mathbf{s}^H\left(\mathbf{I}_M \otimes \mathbf{F}\mathbf{C}_p^H\mathbf{X}\mathbf{X}^H\mathbf{C}_p\mathbf{F}^H\right)\mathbf{s} \\ &= \mathbf{s}^H\mathbf{D}_p\left(\mathbf{X}\right)\mathbf{s}\end{aligned} \tag{17}$$

where $\mathbf{D}_p\left(\mathbf{X}\right) = \mathbf{I}_M \otimes \mathbf{F}\mathbf{C}_p^H\mathbf{X}\mathbf{X}^H\mathbf{C}_p\mathbf{F}^H$.

Substituting (17) into (11), and taking the derivative of the augmented Lagrangian function with respect to the variable $\mathbf{s}^*$, we obtain:

$$\begin{aligned}\frac{\partial\mathcal{L}}{\partial\mathbf{s}^*} = & \sum_{p=0}^{2N-1} 2\mathbf{D}_p\left(\mathbf{x}^{(k+1)}\right)\mathbf{s} \\ & + \rho_u\left(\mathbf{I}_M \otimes \mathbf{F}^H\right)^H\left[\left(\mathbf{I}_M \otimes \mathbf{F}^H\right)\mathbf{s} - \left(\mathbf{x}^{(k+1)} + \mathbf{u}^{(k)}\right)\right] \\ & + \rho_v\sum_{m=1}^{M}\left(\left(\mathbf{I}_M \otimes \mathbf{F}^H\right)^H\mathbf{E}_m^H\mathbf{x}^{(k+1)}\right) \\ & \times\left[\left(\mathbf{x}^{(k+1)}\right)^H\mathbf{E}_m\left(\mathbf{I}_M \otimes \mathbf{F}^H\right)\mathbf{s} - \left(1 - \left(v_m^{(k)}\right)^*\right)\right]\end{aligned} \tag{18}$$

Let the derivative be zero, we can obtain:

$$\begin{aligned}\mathbf{s} = \Bigg[& \sum_{p=0}^{2N-1} 2\mathbf{D}_p \left(\mathbf{x}^{(k+1)}\right) + \rho_u \left(\mathbf{I}_M \otimes \mathbf{F}^H\right)^H \left(\mathbf{I}_M \otimes \mathbf{F}^H\right) \\ & + \rho_v \sum_{m=1}^{M} \left(\mathbf{I}_M \otimes \mathbf{F}^H\right)^H \mathbf{E}_m^H \mathbf{x}^{(k+1)} \\ & \left(\mathbf{x}^{(k+1)}\right)^H \mathbf{E}_m \left(\mathbf{I}_M \otimes \mathbf{F}^H\right)\Big]^{-1} \\ & \times \Big[\rho_u \left(\mathbf{I}_M \otimes \mathbf{F}^H\right)^H \left(\mathbf{x}^{(k+1)} + \mathbf{u}^{(k)}\right) \\ & + \rho_v \sum_{m=1}^{M} \left(\mathbf{I}_M \otimes \mathbf{F}^H\right)^H \mathbf{E}_m^H \mathbf{x}^{(k+1)} \left(1 - \left(v_m^{(k)}\right)^*\right)\Big] \end{aligned} \tag{19}$$

Algorithm 1 summarizes the overall algorithm for solving problem (9) based on the above analysis.

Algorithm 1 ADMM-based Algorithm for solving (9)

Input: The number of BS M, the number of OFDM subcarriers of each BS N, PAPR constraint η, maximum number of iterations K and sidelobe weighting value γ_l
Initialize variables $\mathbf{x}^{(0)}$,$\mathbf{s}^{(0)}$,$\mathbf{u}^{(0)}$,$v^{(0)}$
Set $k = 1$
while
Update $\mathbf{x}^{(k)}$ by solving (15).
Update $\mathbf{s}^{(k)}$ by solving (19).
Update dual variables by
$\mathbf{u}^{(k)} = \mathbf{u}^{(k-1)} + \mathbf{x}^{(k)} - \left(\mathbf{I}_M \otimes \mathbf{F}^H\right)\mathbf{s}^{(k)}$
$v_m^{(k)} = v_m^{(k-1)} + \left(\mathbf{x}^{(k)}\right)^H \mathbf{E}_m \left(\mathbf{I}_M \otimes \mathbf{F}^H\right)\mathbf{s}^{(k)} - 1$
$k = k + 1$.
end while until $k = K$.
Output: optimal waveform $\mathbf{x}$.

IV. Simulation Result

In this section, we will demonstrate the sidelobe performance of the designed collaborative sensing waveform through simulation experiments. The summary of the simulation parameters is given in Table I.

TABLE I: Simulation Parameters

Symbol	Parameter	Value
M	Number of distributed BSs	2
N	Number of OFDM subcarriers of each BS	64
$\mathbf{u}^{(0)}$	Dual variable initial value	0
$v^{(0)}$	Dual variable initial value	0
ρ_u	Penalty factor	100
ρ_v	Penalty factor	10
η	PAPR constraint	2
K	Maximum number of iterations	100
$\gamma_l = 1$	Sidelobe weighting region	$l \in [0, 30]$

Fig. 1 shows the convergence curves of the proposed algorithm. Fig. 1 (left) illustrates the changes in the residual norm and the residual threshold with the number of iterations. From the left figure, it can be observed that the residual norm becomes smaller than the residual threshold after fewer than 100 iterations, satisfying the stopping condition. Moreover, Fig. 1 (right) demonstrates that the objective value in (10) of the proposed algorithm increases monotonically with the number of iterations and finally converges.

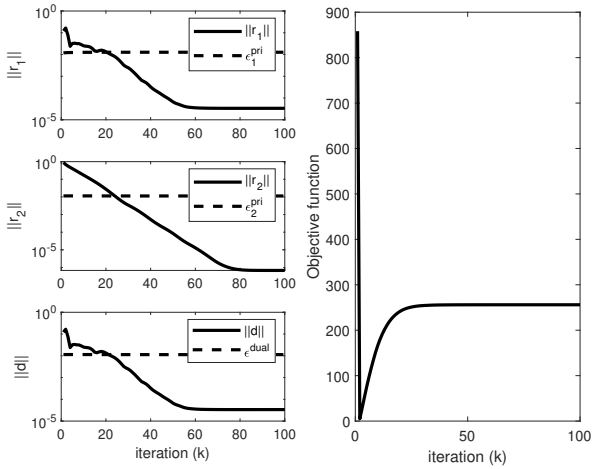

Fig. 1: iteration curve.

Fig. 2 depicts the normalized correlation sidelobe level characteristics of the initial phase random waveform, the algorithm in reference [8] (denoted as constant modulus waveform), and the proposed algorithm. From the simulation results, it can be observed that both the algorithm in reference [8] and the proposed algorithm achieve relatively lower relative sidelobe levels within the region of interest. Moreover, the algorithm proposed in this paper achieves lower relative sidelobe levels compared to the algorithm in reference [8], which is attributed to the additional degree of freedom introduced by the change from the constant modulus condition in the time domain to a PAPR constraint.

Fig.3 shows the characteristic of correlation sidelobe when the weighting factor is $\gamma_l = 1, l \in [0, 10] \cup [30, 50]$. It can be observed that both algorithms achieve lower level within the sidelobe of the interested distance, and the proposed algorithm in this paper achieves lower relative sidelobe level compared to the method in [8].

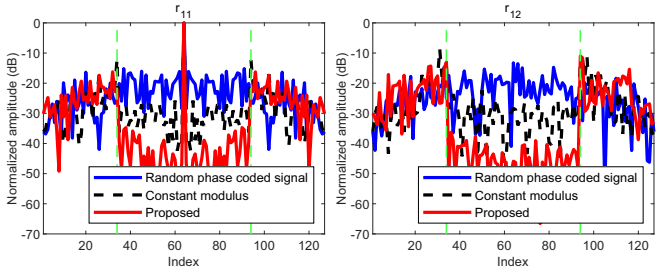

(a) (b)

Fig. 2: Normalized correlation sidelobe level characteristic. (a) r_{11}; (b) r_{12}

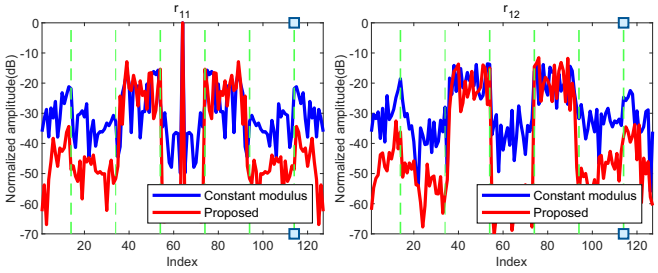

(a) (b)

Fig. 3: The characteristics of normalized relative sidelobe levels under different sidelobe weighting factors. (a) r_{11}; (b) r_{12}

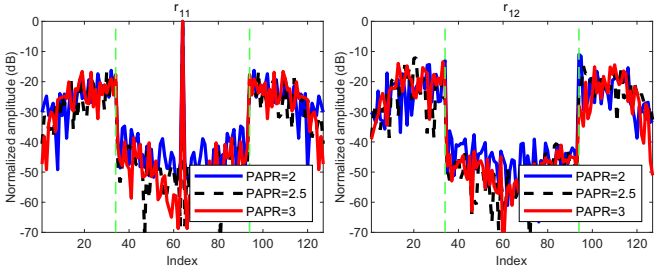

(a) (b)

Fig. 4: The characteristics of normalized relative sidelobe levels under different PAPR. (a) r_{11}; (b) r_{12}

Fig.4 illustrates the characteristics of normalized sidelobe levels under different PAPR values in the same weighting region as Fig.2. The PAPR values are set to 2, 2.5, and 3, respectively. From Fig.4, it can be observed that as the PAPR increases, the normalized sidelobe level decreases. This is because a larger feasible region allows for greater degrees of freedom to be utilized.

V. Conclusion

This paper investigates the waveform design problem for distributed OFDM base stations. Due to the optimization problem being established with a quartic objective function and quadratic equality constraints, it is difficult to obtain a closed-form solution. Therefore, this paper develops a solution based on the ADMM method. The efficiency of the proposed method is verified through simulation experiments, and its performance is compared with existing methods in terms of WISL. The results demonstrate that the proposed method achieves lower WISL compared to the constant modulus waveform design method, thereby proving the effectiveness of the proposed method.

References

[1] H. Deng, "Polyphase code design for orthogonal netted radar systems," *IEEE transactions on Signal Processing*, vol. 52, no. 11, pp. 3126–3135, 2004.

[2] A. M. Haimovich, R. S. Blum, and L. J. Cimini, "Mimo radar with widely separated antennas," *IEEE signal processing magazine*, vol. 25, no. 1, pp. 116–129, 2007.

[3] V. C. Chen and H. Ling, *Time-frequency transforms for radar imaging and signal analysis*. Artech house, 2002.

[4] R. Srinivasan, "Distributed radar detection theory," in *IEE Proceedings F (Communications, Radar and Signal Processing)*, vol. 133, no. 1. IET, 1986, pp. 55–60.

[5] B. Liu, Z. He, J. Zeng, and B. Liu, "Polyphase orthogonal code design for mimo radar systems," in *2006 CIE international conference on radar*. IEEE, 2006, pp. 1–4.

[6] H. He, P. Stoica, and J. Li, "Designing unimodular sequence sets with good correlations—including an application to mimo radar," *IEEE Transactions on Signal Processing*, vol. 57, no. 11, pp. 4391–4405, 2009.

[7] J. Song, P. Babu, and D. P. Palomar, "Sequence design to minimize the weighted integrated and peak sidelobe levels," *IEEE Transactions on Signal Processing*, vol. 64, no. 8, pp. 2051–2064, 2015.

[8] Z. Cheng, B. Liao, Z. He, J. Li, and C. Han, "A nonlinear-admm method for designing mimo radar constant modulus waveform with low correlation sidelobes," *Signal Processing*, vol. 159, pp. 93–103, 2019.

[9] Z. Cheng, Z. He, S. Zhang, and J. Li, "Constant modulus waveform design for mimo radar transmit beampattern," *IEEE Transactions on Signal Processing*, vol. 65, no. 18, pp. 4912–4923, 2017.

[10] B. Nuss, J. Mayer, S. Marahrens, and T. Zwick, "Frequency comb ofdm radar system with high range resolution and low sampling rate," *IEEE Transactions on Microwave Theory and Techniques*, vol. 68, no. 9, pp. 3861–3871, 2020.

[11] B. Nuss, J. Mayer, and T. Zwick, "Limitations of mimo and multi-user access for ofdm radar in automotive applications," in *2018 IEEE MTT-S International Conference on Microwaves for Intelligent Mobility (ICMIM)*. IEEE, 2018, pp. 1–4.

[12] Y.-C. Lin, W.-H. Chung, T.-S. Lee, and Y.-H. Pan, "Non-cooperative interference avoidance in automotive ofdm radars," in *2019 IEEE 89th Vehicular Technology Conference (VTC2019-Spring)*. IEEE, 2019, pp. 1–5.

[13] K. Han, S. Kang, and S. Hong, "Sub-nyquist sampling ofdm radar," *IEEE Transactions on Radar Systems*, vol. 1, pp. 669–680, 2023.

[14] B. Wang, L. Wu, Z. Cheng, and Z. He, "Exploiting constructive interference in symbol level hybrid beamforming for dual-function radar-communication system," *IEEE Wireless Communications Letters*, vol. 11, no. 10, pp. 2071–2075, 2022.

[15] H. Bao, J. Fang, Q. Wan, Z. Chen, and T. Jiang, "An admm approach for papr reduction for large-scale mimo-ofdm systems," *IEEE Transactions on Vehicular Technology*, vol. 67, no. 8, pp. 7407–7418, 2018.

[16] J. He, H. Li, Z. He, W. Wang, and Z. Cheng, "Exploiting base station for remote sensing: Modeling, joint transceiver design, and experiment," *IEEE Transactions on Aerospace and Electronic Systems*, 2024.

[17] Z. Cheng, Z. He, B. Liao, and M. Fang, "Mimo radar waveform design with papr and similarity constraints," *IEEE Transactions on Signal Processing*, vol. 66, no. 4, pp. 968–981, 2017.